Journal of the Chinese Institute of Engineers

ISSN: 0253-3839 (Print) 2158-7299 (Online) Journal homepage: http://www.tandfonline.com/loi/tcie20

Seismic response and stability of underground rock caverns: a case study of Baihetan underground cavern complex

Zhen Cui, Qian Sheng, Xianlun Leng & Jian Chen

To cite this article: Zhen Cui, Qian Sheng, Xianlun Leng & Jian Chen (2015): Seismic response and stability of underground rock caverns: a case study of Baihetan underground cavern complex, Journal of the Chinese Institute of Engineers, DOI: 10.1080/02533839.2015.1066941

To link to this article: http://dx.doi.org/10.1080/02533839.2015.1066941

Published online: 07 Sep 2015.

Journal of the Chinese Institute of Engineers, 2015
http://dx.doi.org/10.1080/02533839.2015.1066941

Seismic response and stability of underground rock caverns: a case study of Baihetan underground cavern complex

Zhen Cui[a,b,c], Qian Sheng[a,c]*, Xianlun Leng[a,c] and Jian Chen[a,c]

[a]*Institute of Rock and Soil Mechanics, Chinese Academy of Sciences, Wuhan, Hubei 430071, P.R. China;* [b]*PowerChina Huadong Engineering Corporation Limited, Hangzhou, Zhejiang 310014, P.R. China;* [c]*State Key Laboratory of Geomechanics and Geotechnical Engineering, Wuhan, Hubei 430071, P.R. China*

(*Received 24 August 2012; accepted 19 August 2014*)

The seismic stability of the underground cavern complex, which houses the Baihetan hydropower plant in Yunnan Province, China, currently the world's 2nd largest underground rock cavern group, is studied in this article. A preliminary performance-based seismic assessment approach specified for underground rock caverns is firstly proposed. The seismic performance objectives are classified. Reference earthquake motions are specified with the determination of the seismic variables. Detailed dynamic response analyses (Method 2B) are conducted based on the parameters given by the cyclic dynamic loading tests with medium strain rate. The seismic response of acceleration, stress, displacement and failure zones are studied. In addition, the seismic spectrum characteristics are analysed with a newly introduced wavelet packet technique. The mechanism of the support measures for seismic stability is also discussed. The assessment for seismic performance of the underground cavern complex is obtained by integrating these results. Serviceability objective of the underground cavern complex under operating basis earthquake may be satisfied, and the safety objective be feasible but with the presence of the proposed reinforcement system. The seismic isolation design is preferred, yet not necessary. And if any seismic isolation design is to be adopted, the frequency absorption range of the isolation material is expected to be 1–4 Hz.

Keywords: underground cavern complex; seismic stability; seismic variable; wavelet packet

1. Introduction

Abundant hydropower resources are available in southwest China, where a number of large-scale hydropower plants are currently either under construction or at design stage. Owing to the mountainous topography in this region, the underground cavern complex is a cost-effective choice, sometimes even the only choice for the powerhouse of a giant hydropower station. Compared with the traditional underground openings such as tunnels, underground caverns are usually very complex in spatial relations owing to the functional requirements. Meanwhile, southwest China is a highly active seismic region with intensive tectonic movements and seismic events, resulting in stringent requirements for seismic design for these hydropower projects. Thus, the seismic stability of large-scale underground cavern complexes is a major geotechnical issue to be addressed during design and construction of these giant hydropower stations.

It is well known that underground structures such as tunnels and caverns are inherently resistant to earthquakes compared to above-ground structures. However, various types of damage are reported in underground structures which have experienced recent strong earthquakes, for instance, the 1976 Tangshan quake (China) (Chinese Ministry of Coal Industry 1982), the 1988 Spitak (Armenia) (Kudoyarov et al. 1989), the 1995 Hyogoken-Nanbu (Japan) (Asakura and Sato 1998), the 1999 Chichi (Taiwan) (Wang et al. 2001), 2007 Singkarak (Indonesia) (Aydan and Genis 2008) and the 2008 Wenchuan (China) (Wang et al. 2009; Li 2011) earthquakes.

As a hydropower plant is usually the major electricity supplier in the region, the failure of an underground powerhouse in an earthquake may also cause secondary disasters to the region by electricity outage. Therefore, the seismic stability of these underground complexes must be seriously addressed.

A variety of studies has been conducted on the seismic assessment of underground caverns. Chang and Seo (1997) suggested a seismic fragility method for underground rock caverns. Dowding, Belytschko, and Dmytryshyn (2000) studied the dynamic stability of a blocky rock cavern under sinusoidal dynamic load. Chen, Chang, and Lee (2004) simulated the stability of the Kukuan underground cavern during the Chichi earthquake, with a discrete element method. Genis and Aydan (2007) and Aydan et al. (2010) studied the formation of yield zones around underground caverns under different

*Corresponding author. Email: cuizhen08@mails.ucas.ac.cn

input ground motions. Zhao and Ma (2009) proposed a reasonable cavern spacing to maintain the stability of the cavern group during earthquakes. Zhang, Xiao, and Chen (2010) conducted an assessment of post-earthquake reinforcement measures of the Yingxiuwan underground powerhouse after the 2008 Wenchuan earthquake.

In spite of the achievements obtained by the previous studies, comprehensive and systematic studies on seismic stability of large-scale underground caverns are rarely reported. Additionally, a streamlining standardized assessment process for seismic response and stability of underground powerhouse complexes is not yet developed. Moreover, spectrum characteristic studies on the response of caverns during an earthquake are not available.

This article aims to establish the seismic assessment process for an underground cavern complex and to introduce a new wavelet packet spectrum characteristics analysis technique. The proposed approach will be applied to a case study, the Baihetan underground cavern complex, currently the world's largest underground rock cavern power station under construction.

2. Project descriptions

The Baihetan hydropower plant is located on the Jinsha River in southwest China. The project site is of typical high-mountain valley topography, as shown in Figure 1. The valley is asymmetrically V-shaped with a higher right bank. The maximum elevation difference between the right and left banks reaches 650 m. The project involved excavation of two large cavern complexes in both left and right banks. Given more unfavourable geological conditions in the right bank, this article will focus on the cavern complex excavated in the right bank.

Figure 1. High-mountain valley topography of the Baihetan hydropower plant project site.

The underground cavern complex consists of the powerhouse, the transformer chamber, the surge chamber, the headrace tunnels, the tailrace tunnels and the auxiliary tunnels. The powerhouse hosts nine generator units with a total capacity of 7 GW. The dimensions of the powerhouse are 439 m × 32.2/29 m × 78.5 m and 400 m × 20.5 m × 33.2 m for the transformer chamber and 321.6 m × 27.6 m × 103.5 m for the surge chamber. The two axes, between the powerhouse and transformer chamber, and between transformer chamber and surge chamber are 77.5 and 72.5 m, respectively.

Figure 2 shows a general perspective of the underground cavern complex.

The overburden depth is approximately 500 m. The existence of three major low-angled faults was detected, as shown in Figure 3. These faults are identified as C3, C4 and C5. Their orientation is approximately 135°/20°, in which 135° is the dip direction and 20° is the dip angle. The surrounding rock masses are mainly aphanitic basalt, amygdaloidal basalt and brecciated lava. The mechanical parameters of the rock mass are shown in Table 1. The *in situ* stress field near the cavern complex is strongly influenced by the topography and tectonic activities. According to the *in situ* stress measurement results, the fitting formulae for principal stresses given in Equation (1) can be used to estimate the stress field. In which σ_H is nearly north-south, and σ_v is in a vertical direction. The principal components of the *in situ* stress field in the vicinity of the cavern complex were recorded approximately as 22, 14 and 8 MPa, respectively.

$$\begin{cases} \sigma_v = 0.0254 \times H \\ \sigma_H = 0.0374 \times H + 2.4648 \\ \sigma_h = 0.0207 \times H + 1.3962 \end{cases}, \quad (1)$$

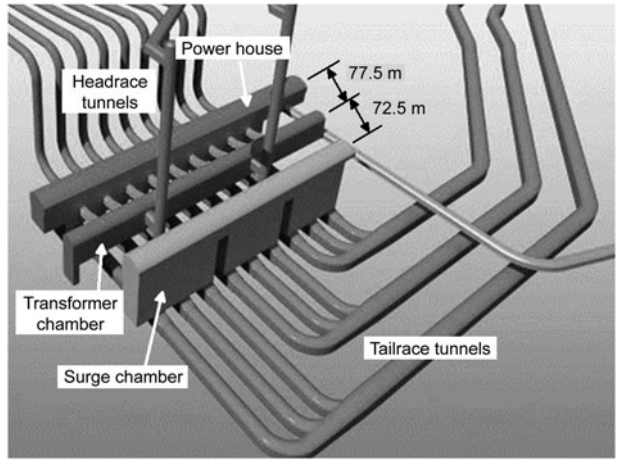

Figure 2. General perspective of the cavern complex.

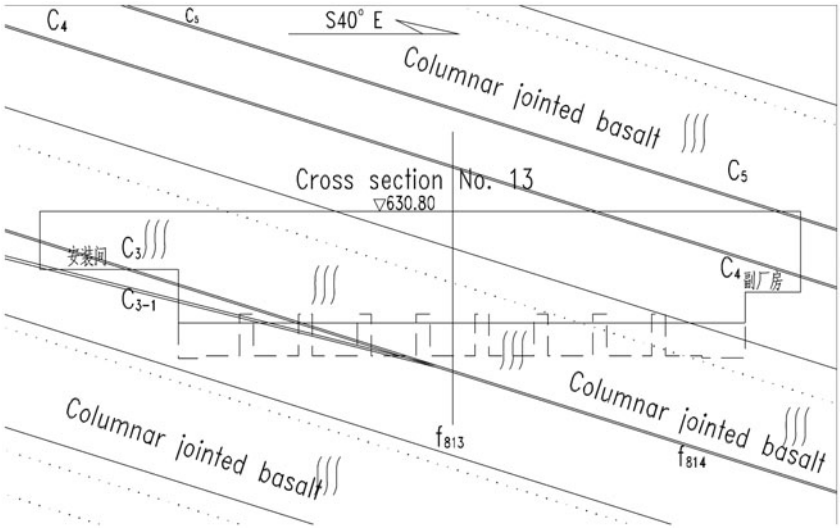

Figure 3. Plan view of the powerhouse cavern.

Table 1. Mechanical parameters of the surrounding rock masses and the faults.

Rock type	Unit weight (kg/m^3)	Deformation modulus (GPa)	Poisson's ratio	Cohesion (MPa)	Friction angle (°)	Tensile strength (MPa)
Ⅱ	2800	15	0.23	2.5	53.5	0.5
Ⅲ	2700	10	0.25	2.2	48.2	0.4
C3, C5	2350	0.9	0.35	0.4	18.3	0.2
C4	2350	0.7	0.35	0.3	16.7	0.1

where σ_v is the vertical stress (σ_2), measured in MPa. σ_H is the maximum horizontal stress (σ_1), measured in MPa. σ_h is the minimum horizontal stress (σ_3), measured in MPa. And H is the overburden depth, measured in m.

3. Principles and procedure

3.1. *Principles*

A preliminary performance-based seismic assessment approach specified for underground rock caverns is proposed here, following the existing International Standard ISO23469: 2005 Bases for design of structures – Seismic actions for designing geotechnical works (ISO 2005). In the performance-based approach, the objective of seismic design is defined in accordance with the function and importance of the engineering structure, for instance, for commercial, public or emergency use. In this study, the Baihetan HPP is one of the key points of China's West-East Electricity Transmission Project, and has been classified as a class I project, the most vital rank according to the Chinese code.

Currently, Chinese seismic codes for hydropower projects are based on a single-level design concept. Only a probability level of 5% in 50 years ($p_{50} = 5\%$) is specified for seismic design of underground cavern complexes. Hence, they are not applicable to the performance-based approach which involves multi-level ground motions. International Standard ISO23469: 2005 specifies a two-level seismic assessment for geotechnical structures. And after the killer earthquake of Wenchuan 2008, an interim regulation has been issued by Chinese authority (Hydropower and Water Resources Planning and Design General Institute 2008) that a two-level seismic stability assessment shall be performed for the critical components of large-scale hydropower plants. In this manner, the reference ground motions may be set into two levels. The exceedance probability is set to be $p_{50} = 5\%$ and $p_{100} = 2\%$, in accordance with the most common results by a probabilistic seismic hazard analysis (PSHA) and the current codes. The two levels of ground motion are named as the term of operating basis earthquake (OBE) and safety evaluation earthquake (SEE), respectively.

For each ground motion level mentioned above, the performance levels are then specified for seismic performance assessment of the cavern complex as follows:

Serviceability during and after an earthquake: minor impact to electricity generating function, or with function unimpaired and economically recoverable after temporary disruption, the caverns may experience acceptable

Table 2. Combination of earthquake motion and seismic performance level.

Earthquake motion	Performance required	
Operating basis earthquake (OBE)	Serviceability	Safety
Safety evaluation earthquake (SEE)		Safety

seismic deformation, the surrounding rock and the supporting structures may suffer minor damage; safety during and after an earthquake: personnel casualties and damage to installed equipment shall be minimized, while the key equipment such as the generators shall be repairable, and the caverns shall not collapse.

The seismic performance levels corresponding to different earthquake motion levels are shown in Table 2.

3.2. *Procedure for dynamic response analysis*

Four analysis methods are given in International Standard ISO23469:2005 for obtaining the response of a structure to earthquake motion. The methods may be broadly categorized as simplified equivalent static (Method 1A), detailed equivalent static (Method 1B), simplified dynamic (Method 2A) and detailed dynamic (Method 2B). In this case study, Method 2B is adopted, as requested for a Class I project by the design code, and in the understanding that the use of a more sophisticated method may lead to better profit. A flow chart of the performance-based seismic assessment (Yukio and Tsutomu 2003) now can be established following Clauses 5–9 of International Standard ISO23469: 2005 (Figure 4).

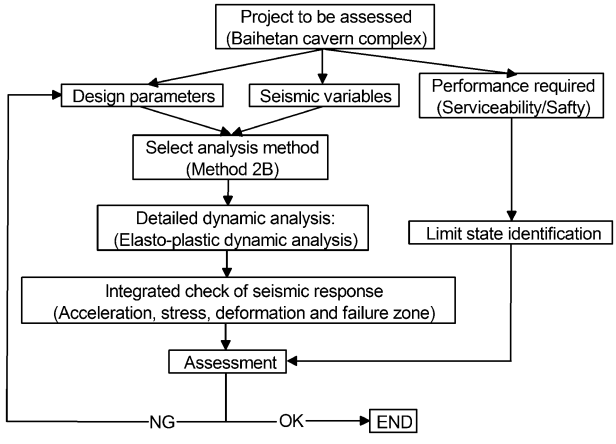

Figure 4. Flow chart of the performance-based seismic assessment approach.

4. Determination of seismic variables

An exhaustive PSHA has been carried out by China Earthquake Administration as the code requested for a Class I project as the Baihetan HPP (hydropower plant). A basic earthquake intensity VIII is obtained, and the reference earthquake motion parameters are given, as shown in Table 3 and Figure 5.

No strong seismic motion was recorded in the history near the project site. Thus, a specified technique of artificial simulation of non-stationary seismic motion for large-scale underground cavern complex (Zhang et al. 2009) was conducted. The simulated wave forms for OBE and SEE are shown in Figure 6.

According to Chinese seismic codes, a discount factor of 2 is specified for the peak acceleration value in the seismic analysis of underground structures with overburden depth greater than 50 m. Therefore, the peak values of OBE and SEE are set to be 109 and 170 gal in the following analyses, respectively. And the vertical component of the accelerograms was taken as two-thirds of the horizontal component, during the following analysis. During the numerical simulation, the earthquake wave form was the input from the bottom of the model to simulate the propagation of the ground motion.

5. Detailed dynamic response analysis

In this case study, the elasto-plastic model was employed to perform the detailed dynamic analysis (Method 2B),

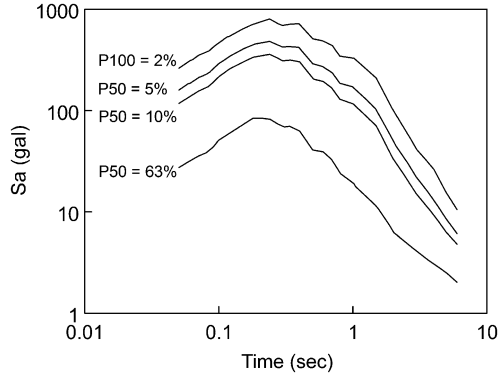

Figure 5. Response spectra specified for the project site.

Table 3. Reference earthquake motion parameters of the Baihetan hydropower plant.

Probability of exceedance	$p_{50}=63\%$	$p_{50}=10\%$	$p_{50}=5\%$	$p_{100}=2\%$
Peak ground acceleration (gal)	51	165	219	340

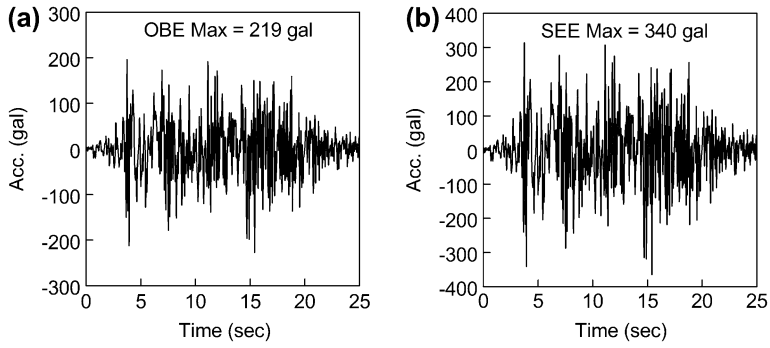

Figure 6. Waveform of simulated OBE and SEE.

with the mechanical parameters shown in Table 1 and a Mohr-Coulomb criterion with an elastic-perfectly plastic law. In addition, the support measures were also taken into consideration. A support system consisting of rock bolt and mesh reinforced shotcrete for the static condition was designed by PowerChina Huadong Engineering Corporation Limited (Previously known as ECIDI), as shown in Figure 7. In the numerical simulation, bolt and mesh reinforced shotcrete are both simulated as elastic materials for simplicity. The modulus of elasticity for the bolts and mesh is set as 200 GPa as the elasticity modulus of steel material. The corresponding Poisson's ratio is 0.3. And the modulus of elasticity for the shotcrete is set as 30 GPa for the type C30 concrete. The corresponding Poisson's ratio is 0.2.

A two-dimensional numerical model was established for cross section No.13 (see Figure 3) of the underground cavern complex which was thought to be the most unfavourable section both related to excavation and in seismic terms, as illustrated in Figure 8. The *in situ* stress field was implemented based on Equation (1). The fault zone was modelled as a layer of finite difference zones with gauge material as the mechanical parameters

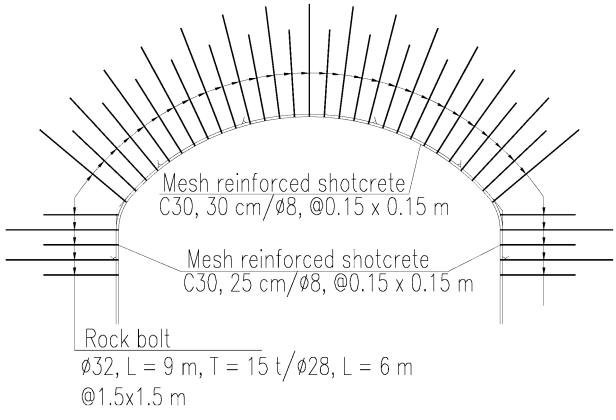

Figure 7. Reinforcing measures of the underground caverns.

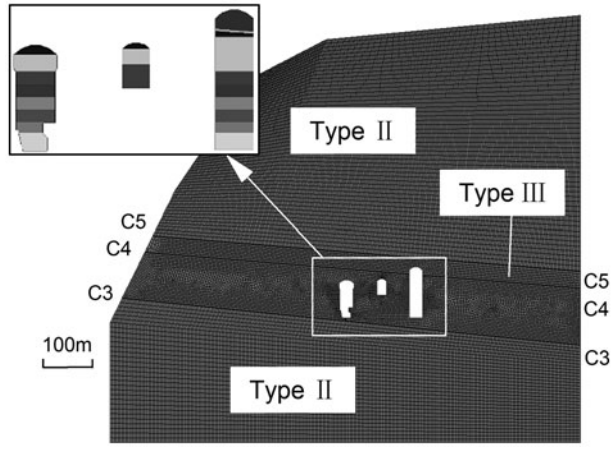

Figure 8. Geometry and FE mesh of cross section No.13, and the excavation stages.

shown in Table.1. The caverns were excavated from the top arch and followed by benching down in seven stages to excavate the body of the caverns. The layout of key points in the numerical model is shown in Figure 9. The analysis was performed with the FLAC3D code developed by Itasca (Itasca 2005). An average size of 8 m was adopted in consideration of the strict requirements on element sizes in the dynamic analysis. And free-field boundary conditions and Rayleigh damping were used.

In order to verify the performance of the reinforcement system during earthquakes, four cases were considered for analysis, as shown in Table 4.

The acceleration responses, stress responses, displacements and rock mass failure zones are studied, respectively.

5.1. *Acceleration responses*

The peak acceleration responses of the key points are listed in Table 5. The maximum responses take place at the bottom of the caverns and the exposed fault zones,

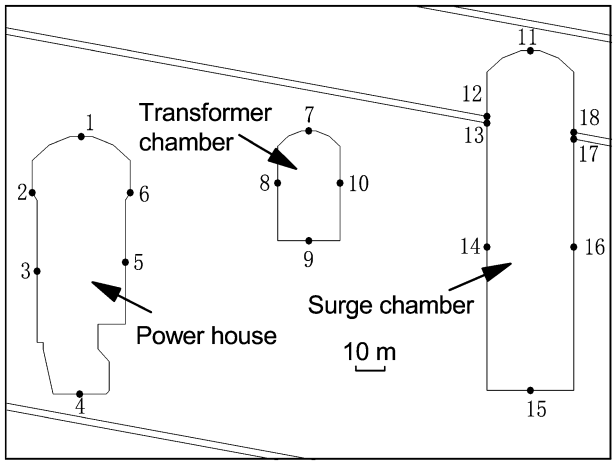

Figure 9. Layout of the key points.

Table 4. Analysis cases for two-dimensional elasto-plastic dynamic analysis.

Earthquake level	Unsupported	Supported
OBE	A1	B1
SEE	A2	B2

Table 5. Peak acceleration responses of the key points (Unit: gal).

Key pts.	1	2	3	4	5	6	7	8	9
A1	78	88	132	110	125	137	100	119	103
B1	53	122	100	109	90	87	71	103	103
A2	151	190	172	179	171	246	158	197	243
B2	122	169	124	214	208	206	121	183	170
Key pts.	10	11	12	13	14	15	16	17	18
A1	110	90	196	84	101	104	72	88	84
B1	129	74	152	89	155	104	143	93	78
A2	255	156	259	269	228	186	152	170	154
B2	197	132	202	220	221	194	133	168	134

while the responses at cavern crowns are relatively slight. This tendency can be observed in all four cases under study.

For the OBE cases (A1 and B1), the maximum responses are approximately 1.2 times higher than that of the peak input. For the SEE cases (A2 and B2), this ratio increases to approximately 1.4, indicating the non-linear nature of the response.

Comparing A cases and B cases, the presence of support measures does help to reduce the acceleration responses, to a certain degree. This may be due to the interlocking and self-supporting arch effect by the pattern support.

Figures 10 and 11 show the acceleration responses at the key points 1 and 4.

5.2. *Stress responses*

Figure 12 shows the stress field around the cavern complex after excavation, without/with support measures. Stress concentrations in the upstream spring line of the powerhouse and the bottom of the downstream side wall of the surge chamber are relieved when the caverns are supported.

Figure 13 shows the stress field around the cavern complex after earthquake for each case. Under the action of the dynamic load due to earthquake, stress loss can be observed in the stress distribution around the opening after earthquake. As the earthquake intensity increases, the stress loosening phenomenon correspondingly becomes more marked. The stress loosening is assumed to be caused by the residual deformation owing to the non-linear behaviour of the rock mass under dynamic loading.

Figures 14 and 15 show the time histories of stress responses at the crown and the bottom of the powerhouse cavern. The gradual decrease of major and minor principal stresses corresponds well with the stress release

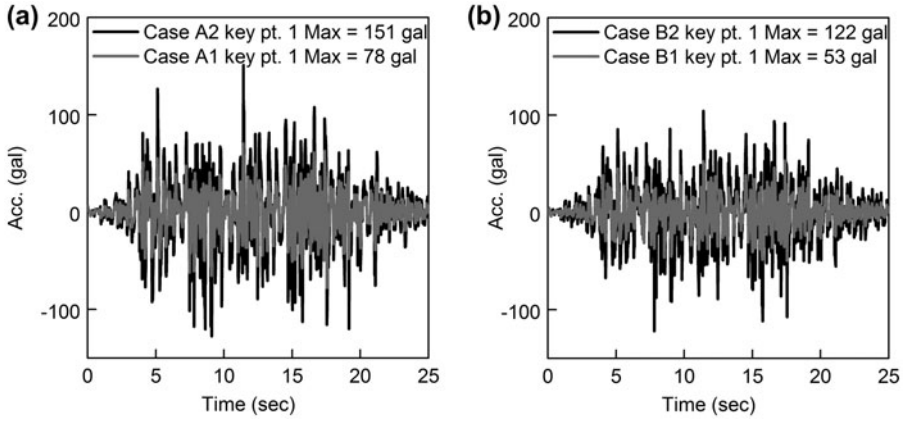

Figure 10. Acceleration responses at the crown of the powerhouse cavern (key pt.1).

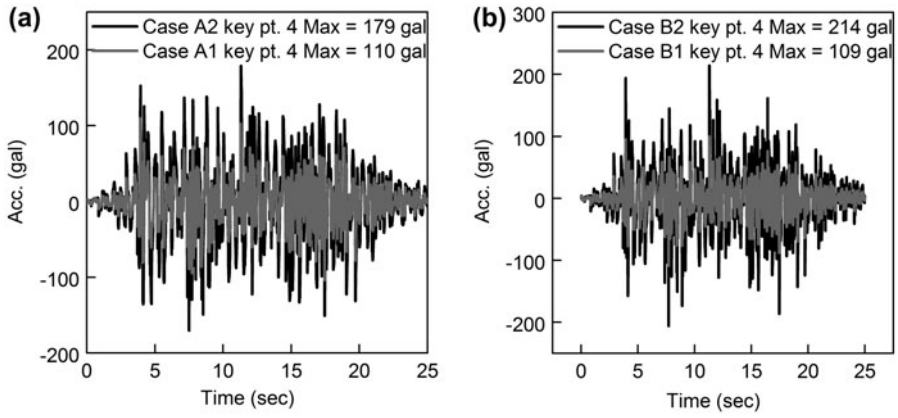

Figure 11. Acceleration responses at the crown of the powerhouse cavern (key pt.4).

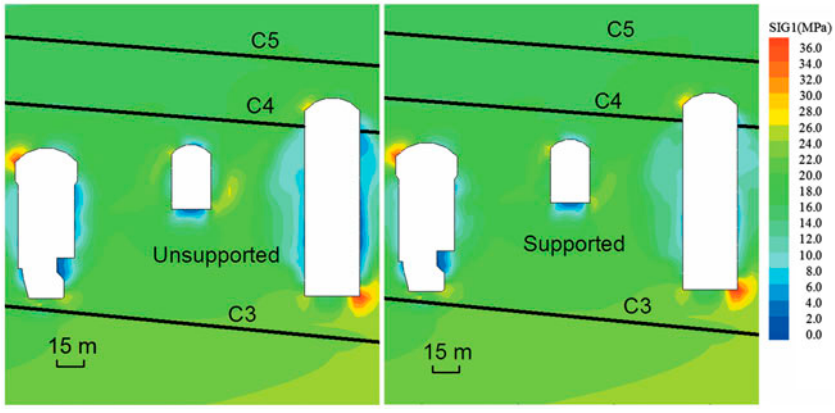

Figure 12. Stress field around caverns after excavation, without/with support measures (MPa).

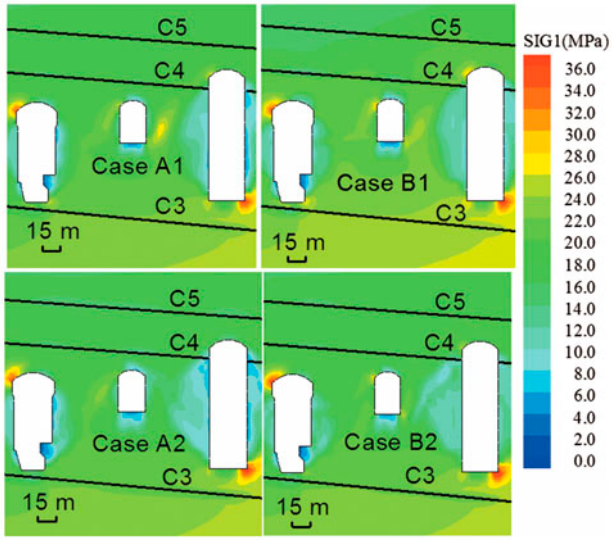

Figure 13. Stress field around caverns after earthquake (MPa).

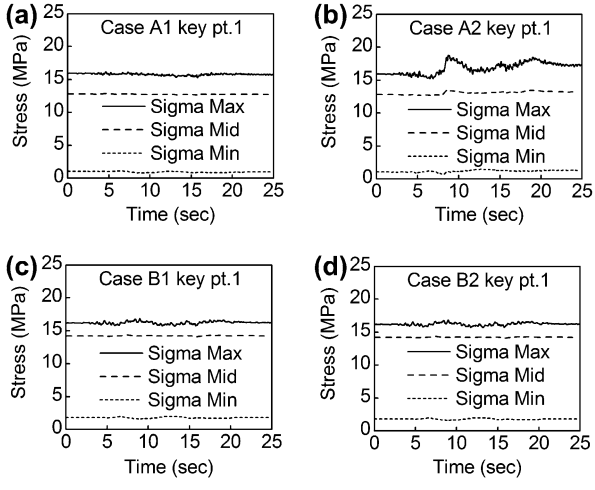

Figure 14. Stress responses at the crown of the powerhouse cavern (key pt.1).

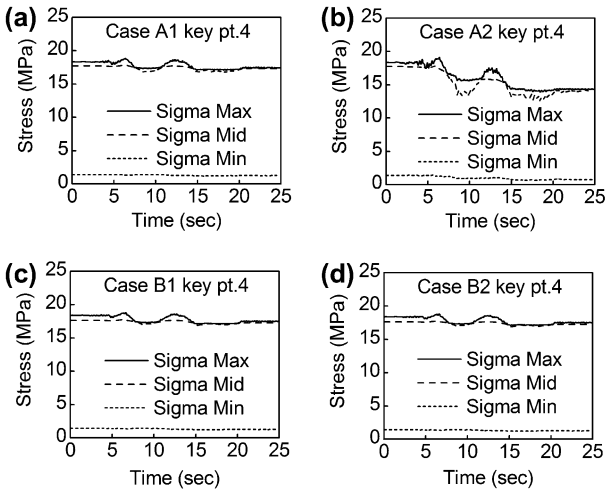

Figure 15. Stress responses at the bottom of the powerhouse cavern (key pt.4).

shown in Figure 13. The large fluctuation of the major principal stress in Case A2 indicates the probable failure of rock mass. The relatively "smooth" time history curves in Case B1 and Case B2 indicate seismic stability in the presence of the support system.

5.3. *Displacement*

Figure 16 shows the displacement contours after excavation, without/with support measures. The support system can help to reduce the deformation around the caverns.

Figure 17 shows the seismic displacement contours after earthquake for each case. As the earthquake intensity increases, the seismic displacement increases correspondingly. Furthermore, with the presence of support system, the maximum incremental displacement is reduced from 12 cm in Case A2 to 10 cm in Case B2.

Figure 18 shows the time histories of relative displacement at the key points and the deformation mode

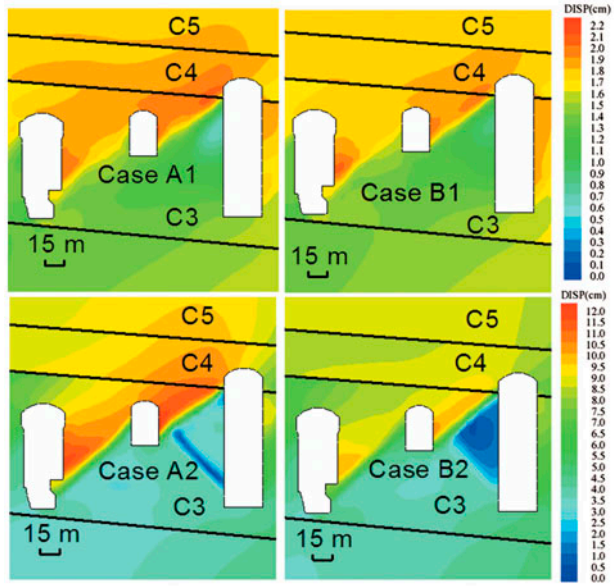

Figure 17. Seismic displacement contour after earthquake (cm).

corresponding to the peak relative displacement. The peak relative displacements take place almost simultaneously. The deformation modes of the caverns are nearly wholly shear deformation, or first-order vibration mode, in structural dynamics terms.

Once again, the "non-convergent" relative displacement curve in Case A2 indicates the potential failure of rock mass in this case. The supported cavern complex (Cases B1 and B2) proves to be very stable after earthquake.

5.4. *Failure of rock mass*

In this section, the stability of the cavern complex is evaluated with the failure zone development. One of the

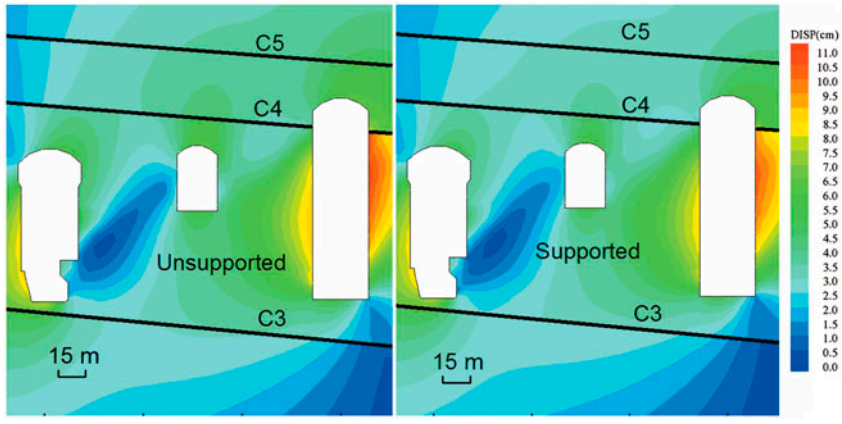

Figure 16. Deformation contour after excavation, without/with support measures (cm).

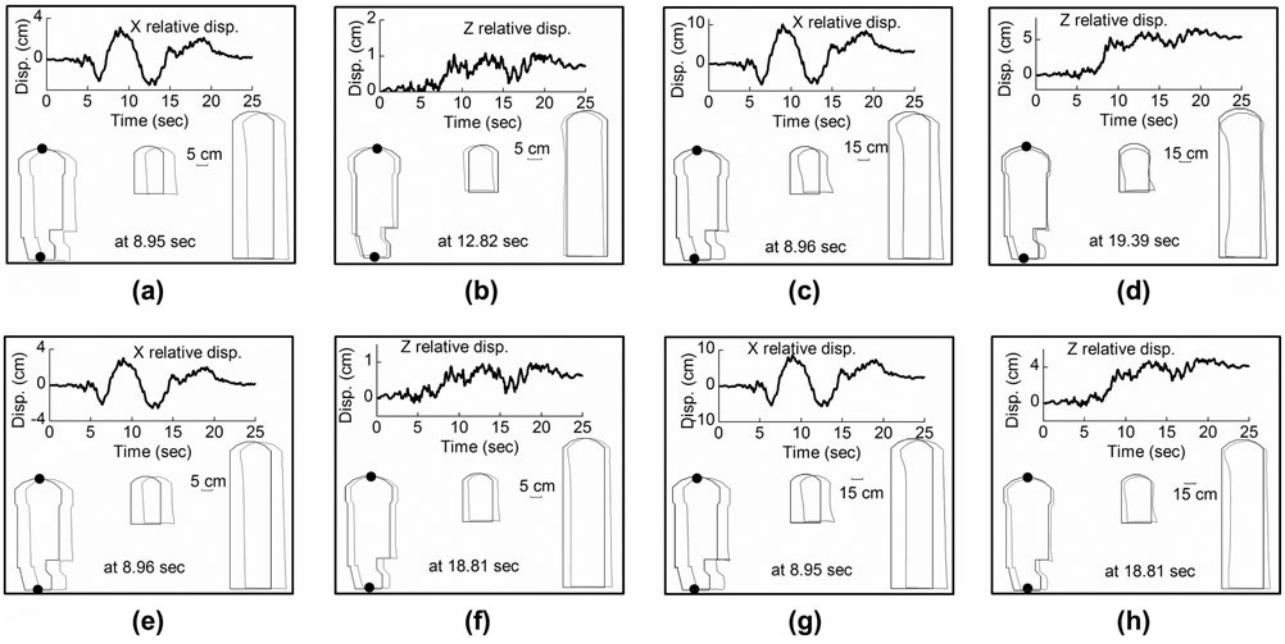

Figure 18. Time histories of relative displacement between the crown and the bottom and deformation shape corresponding to the peak displacement.

major problems in elasto-plastic seismic analyses is the estimation of the dynamic strength properties of the rock mass. In order to determine the indicator of failure under seismic loading, triaxial cyclic loading dynamic tests with medium strain rate have been conducted on 12 specimens.

As the Predominant Period of an earthquake is usually around 1 s, the rock mass experiences a low-frequency cyclic loading during an earthquake, which exhibits different mechanical behaviours compared to the traditional dynamic loading cases, such as that of an explosion. The frequency of the cyclic loading was set to be 1 Hz to simulate the seismic load. The tests were performed with a rock mechanics testing machine RMT-150C developed by the Institute of Rock and Soil Mechanics, the Chinese Academy of Sciences (WHRSM). The details of the test will not be presented here due to the limited length of this article. As to the findings of the test, it was found that the plastic strain gradually accumulates with the number of loading cycles, and the specimen crushes subsequently as the cyclic plastic strain reaches a critical threshold. Thus, this threshold value is termed critical cyclic plastic strain and taken as the indicator of failure. The test results indicate that the mean critical cyclic plastic strain is about $0.5e^{-4}$. The failure zones are then determined according to this critical cyclic plastic strain.

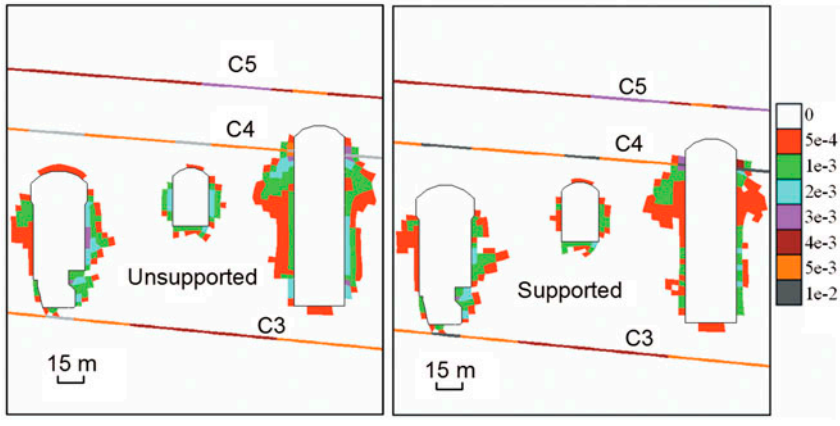

Figure 19. Failure zones and plastic strain contours after excavation, without/with support measures.

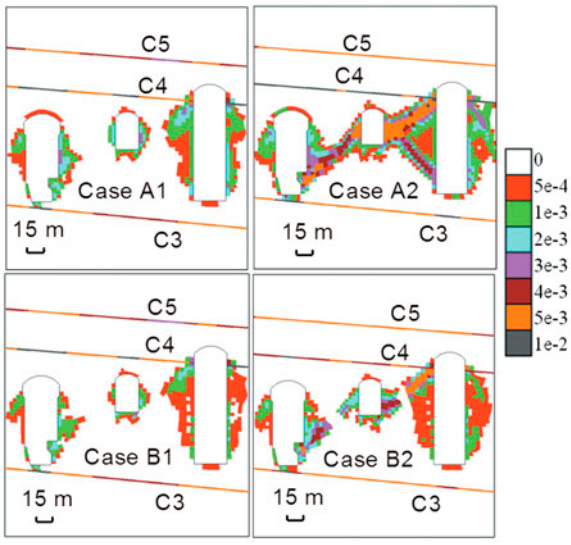

Figure 20. Failure zones and plastic strain contours after earthquake.

Figure 19 shows the failure zones and the plastic strain contours after excavation in the surrounding rock mass without/with support measures. Figure 20 illustrates the failure zones and the plastic strain contours after earthquake for each case. As the earthquake intensity increases, the area of failure zones correspondingly increase, and they tend to run through the rock pillars between caverns. In Case A2, the failure zones have run through both rock pillars. This situation probably corresponds to a state of total collapse of the underground cavern complex, in which the necessity of a proper support system emerged. In Case B2, with the help of the designed support system, the failure zones were restricted to a critical yet acceptable state. In this manner, the seismic stability of the cavern complex may be insured.

5.5. *Spectrum characteristics*

A spectrum characteristics analysis was carried out based on a newly introduced wavelet packet technique. The wavelet method is an innovative signal process tool for time-frequency analysis, compared with the traditional Fourier methods. Wavelet analysis consists of decomposing a signal into a hierarchical set of approximations and details. The levels in the hierarchy often correspond to those in a dyadic scale. From the signal analyst's point of view, wavelet analysis is a decomposition of the signal from family of analysed signals, which is usually

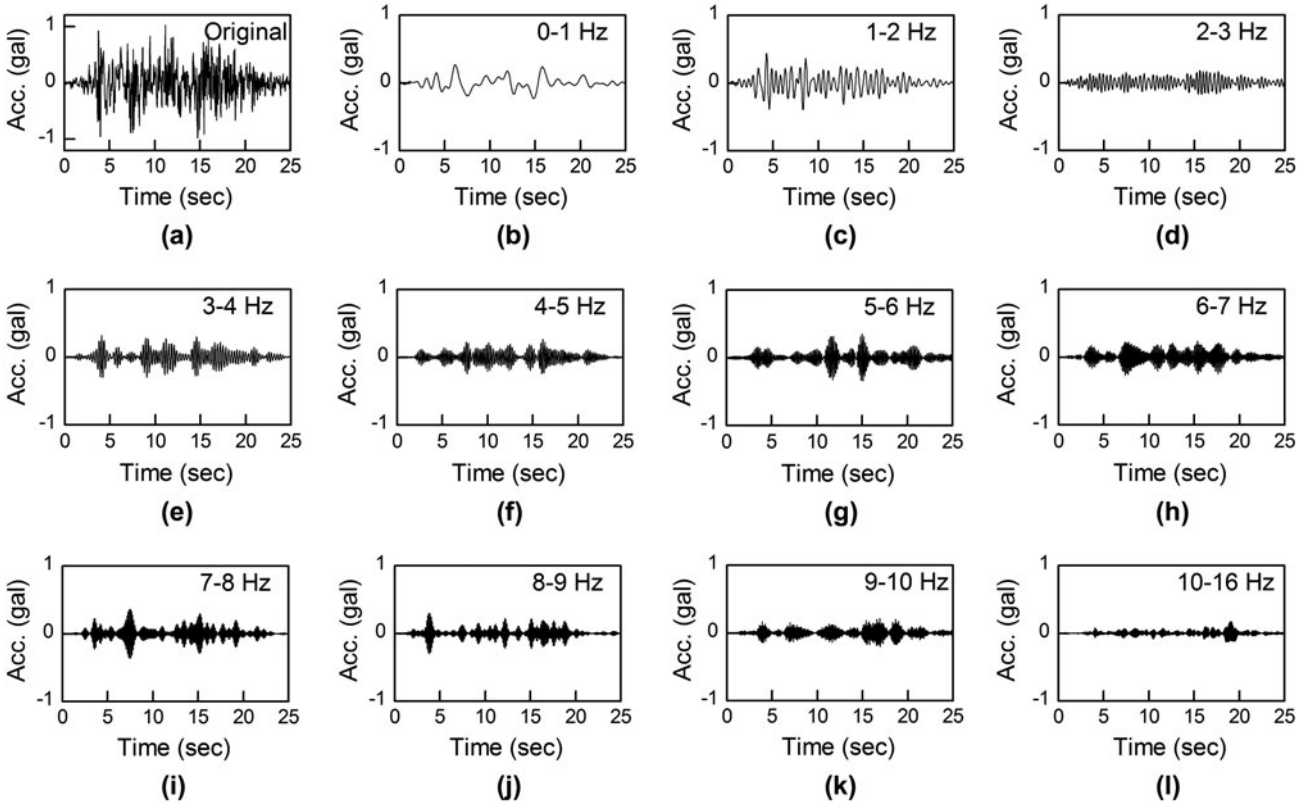

Figure 21. Original normalized OBE wave form and the wavelet coefficients.

an orthogonal function method. From an algorithmic point of view, wavelet analysis offers a harmonious compromise between decomposition and smoothing techniques (The MathWorks 2010).

The wavelet packet method is a generalization of wavelet decomposition that offers a rich range of possibilities for signal analysis. It provides multi-level division of the frequency band, and further decomposition for the high-frequency part that the wavelet methods may not deal with.

The normalized OBE wave form is decomposed with the wavelet packet method as an example. The original wave form and the wavelet coefficients are shown in Figure 21.

Here, the acceleration responses are decomposed into different frequency bands. The Arias Intensity of each wavelet coefficient is then derived to reveal the dominant influential frequencies (Cui et al. 2010). The distinct-frequency-banded distributions of Arias Intensity at the bottom and crown of the powerhouse cavern in each case are shown in Figure 22.

The results show that during the upward propagation of a seismic wave, different frequency components may not follow similar trends. High-frequency components are more likely to be absorbed during wave propagation. Although perplexing and confusing results emerged due to the non-linear properties of the rock mass and the support system, a dominant influential frequency band of

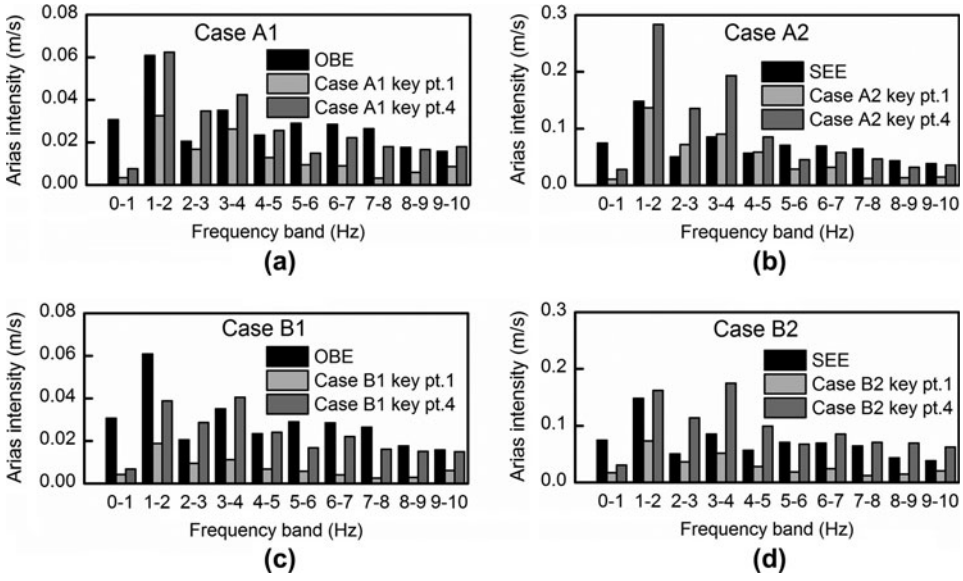

Figure 22. Distinct-frequency-banded distributions of Arias intensity at the bottom and crown of the powerhouse cavern.

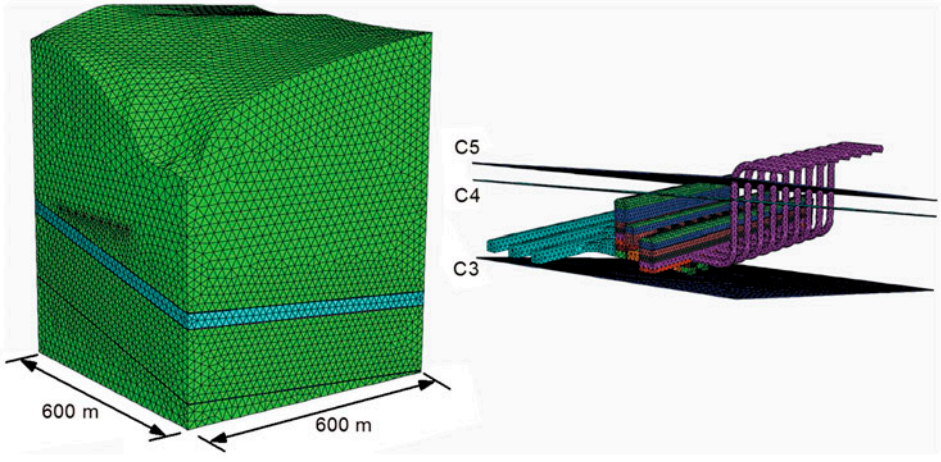

Figure 23. FE mesh of the full three-dimensional model.

1–5 Hz is obtained for the bottom, particularly 1–3 Hz, and that for the crown is 2–4 Hz.

Thus far, the nature of the spectrum characteristics of the caverns is revealed. The caverns are quite sensitive to seismic waves with frequency in the range of 1–4 Hz. Therefore, if any seismic isolation design is to be adopted, the absorption range of the isolation material is expected to be 1–4 Hz. In addition, the support system affects the dynamic characteristics of the caverns, leading to dynamic responses with more high-frequency components. The reason for this phenomenon may be explained as that the installation of support measures increasing the stiffness of the rock mass, and consequently the Eigen frequency (frequency that represents the dynamic characteristic). Fortunately, this phenomenon may be less important as the high-frequency components of the seismic wave generated by an earthquake are usually not abundant, but may provide certain references in the dynamic design of the hydroelectric machinery installed inside the caverns.

5.6. *Three-dimensional elasto-plastic dynamic analysis*

A final computation is carried out, with a sophisticated three-dimensional elasto-plastic model, as shown in Figure 23.

Due to the strict requirements on element sizes in the dynamic analysis and the resulting massive amount of elements, the full 3-D dynamic computation is time-consuming even with powerful workstations and parallel processing. Thus, only 2 cases were set up, C1 and C2, corresponding to the above Case B1 and Case B2. Generally, the results of 3-D analysis are in good agreement with those of 2-D analysis. Therefore, it is not necessary to present those results here.

Figure 24 shows the failure zones and the plastic strain contours of Cross Section No.13 after earthquake for each case, and the horizontal profile of the failure zones. These results reveal, unambiguously, the intact state of caverns under OBE, and a disturbed but safe state under SEE.

5.7. *Discussions*

From the above analyses, an integrated assessment for seismic performance of the Baihetan cavern complex can be made.

Under OBE, the seismic displacement of the underground caverns is within an acceptable limit of less than 2 cm, the stress field around caverns is essentially unchanged, and the failure of the surrounding rock mass is negligible. The serviceability and safety objectives of the underground cavern group under OBE can be satisfied, even with no support measure.

When it comes to SEE, if the caverns are unsupported, the seismic displacement may be unacceptable, the stress field around caverns is violently disturbed and the failure zones tend to run through both rock pillars, suggesting a state of total collapse of the underground cavern complex. Nevertheless, if a proper support system is implemented, the rock mass failure may be controlled within a critical state. The caverns may suffer severe damage; however, collapse is not likely to occur. That is, the safety objective can be fulfilled with the proposed support system. The seismic isolation design is preferred, yet not necessary.

According to the seismic spectrum characteristics analysis, the caverns are quite sensitive to seismic waves of 1–4 Hz. Therefore, if any seismic isolation design is to be adopted, the absorption range of the isolation material is expected to be 1–4 Hz.

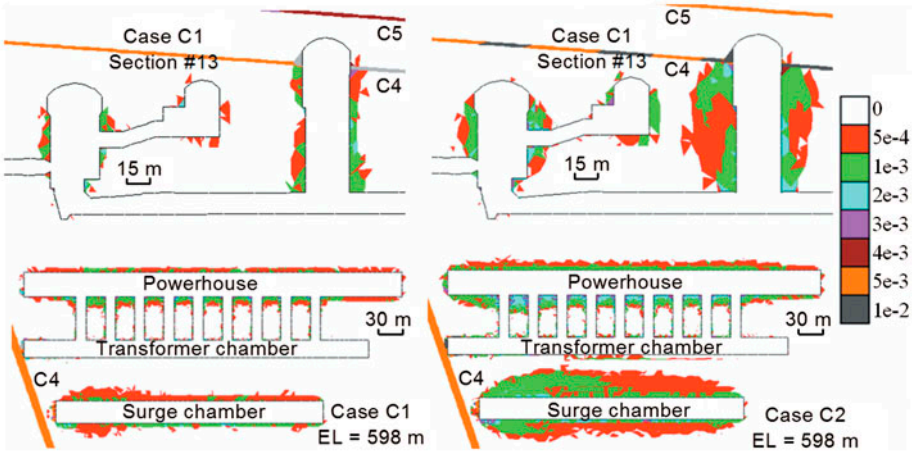

Figure 24. Failure zones and plastic strain contours after earthquake.

6. Summary

This article provides the framework of a performance-based seismic assessment approach specified for underground rock caverns. A case study has been carried out to illustrate the application of the proposed approach. The main results of this article may be summarized as follows:

(1) A procedure for the seismic assessment is established following International Standard ISO23469: 2005. The performance objectives are classified based on the function and importance of the cavern as serviceability and safety. Reference earthquake motions are specified for each objective relative to OBE and SEE conditions. The detailed dynamic method (Method 2B) is adopted for analysis.

(2) The seismic variables of the Baihetan hydropower plant project were firstly determined for the OBE and SEE. The wave forms for the dynamic analysis were simulated.

(3) Detailed dynamic response analysis was conducted for the Baihetan underground cavern complex, with both 2-D and 3-D full elasto-plastic models, based on the parameters given by the cyclic loading dynamic tests with medium strain rate on 12 specimens. The acceleration, stress, displacement and failure zones during and after earthquake were studied. The spectrum characteristics were also analysed by a newly introduced wavelet packet technique. The mechanism of the support measures for seismic stability is also discussed.

(4) The assessment for seismic performance of the Baihetan underground cavern complex was obtained. The serviceability and safety objectives of the underground cavern complex under OBE may be satisfied with or without support measures, and the safety objective under SEE is feasible, given the proposed support system. The seismic isolation design is preferred, yet not necessary.

(5) The nature of the spectrum characteristics of the caverns is revealed via wavelet packet technique. According to the seismic spectrum characteristics of the cavern complex, if any seismic isolation design is to be adopted, the frequency absorption range of the isolation material is expected to be 1–4 Hz.

Nomenclature

EL	elevation
Gal	Galileo
GPa	Giga-Pascal
H	overburden depth
Hz	Hertz
kg	Kilogram
m	Meter
MPa	Mega-Pascal
OBE	operating basis earthquake
PSHA	probabilistic seismic hazard analysis
SEE	safety evaluation earthquake
σ_1	maximum principal stress
σ_2	intermediate principal stress
σ_3	minimum principal stress
σ_H	maximum horizontal stress
σ_h	minimum horizontal stress
σ_v	vertical stress
°	degree symbol

Disclosure statement

No potential conflict of interest was reported by the authors.

Funding

This work was financially supported by the National Basic Research Program of China [grant number 2015CB057905]; National Natural Science Foundation of China [grant number 51409263], [grant number 11472292]; China Postdoctoral Science Foundation [grant number 2014M561736].

References

Asakura, T., and Y. Sato. 1998. "Mountain Tunnels Damage in the 1995 Hyogoken-Nanbu Earthquake." *Quarterly Report of Railway Technical Research Institute* 39 (1): 9–16.

Aydan, Ö., and M. Genis. 2008. "The Seismic Effects on the Bukit-Tinggi WWII Underground Shelter by 2007 Singkarak (Solok) Earthquake." In *Proceedings of the ISRM International Symposium 2008, Fifth Asian Rock Mechanics Symposium*, Tehran, Iran, 24–26 November 2008: 917–924. Salzburg: International society of Rock Mechanics.

Aydan, Ö., Y. Ohta, M. Geniş, N. Tokashiki, and K. Ohkubo. 2010. "Response and Stability of Underground Structures in Rock Mass during Earthquakes." *Rock Mechanics and Rock Engineering* 43 (6): 857–875. doi: 10.1007/s00603-010-0105-6.

Chang, S. P., and J. M. Seo. 1997. "Seismic Fragility Analysis of Underground Rock Caverns for Nuclear Facilities." In *Transaction of the 14th International Conference on Structural Mechanics in Reactor Technology*, Lyon, France, 17–22 August 1997. Vol. 10: 151–158. Raleigh, NC: SMiRT.

Chen, J. C., Y. L. Chang, and H. C. Lee. 2004. "Seismic Safety Analysis of Kukuan Underground Power Cavern." *Tunnelling Underground Space Technology* 19 (4–5): 516–527. doi: 10.1016/j.tust.2004.02.110.

Chinese Ministry of Coal Industry, Coal Mines Planning and Design Institute. 1982. "Damage to Structures and

Installations in the Underground Excavations of the Kailuan Colliery during the Tangshan Earthquake." *Earthquake Engineering and Engineering Vibration* 2 (1): 67–77. (in Chinese).

Cui, Z., Q. Sheng, J. J. Liu, and X. L. Leng. 2010. "Spectrum Characteristics Analysis of Seismic Response for Underground Houses via Wavelet Packet." *Rock and Soil Mechanics* 31 (12): 3525–3530. (in Chinese). doi: 10.3969/j.issn.1000-7598.2010.12.033.

Dowding, C. H., T. B. Belytschko, and O. Dmytryshyn. 2000. "Dynamic Response of Million Block Cavern Models with Parallel Processing." *Rock Mechanics and Rock Engineering* 33 (3): 207–214. doi: 10.1007/s006030070007.

Genis, M., and Ö. Aydan. 2007. "Static and Dynamic Stability of a Large Underground Opening." In *Proceedings of the Second Symposium on Underground Excavations for Transportation*, Istanbul, Turkey, 15–17 November 2007: 317–326. Istanbul: TMMOB. (in Turkish).

Hydropower and Water Resources Planning and Design General Institute, HydroChina. 2008. *Interim Regulation for Seismic Design and Special Reports Preparation of Hydropower Projects (No. 2008-24)*. Beijing: Hydropower and Water Resources Planning and Design General Institute, HydroChina.

ISO (International Organization of Standardization) 2005. *Bases for Design of Structures – Seismic Actions for Designing Geotechnical Works*. ISO23469-2005. Geneva: International Organization of Standardization.

Itasca Consulting Group. 2005. *FLAC3D (Fast Lagrangian Analysis of Continua in 3D) Optional Features (version 3.0)*. Minneapolis: Itasca Consulting Group.

Kudoyarov, L. I., G. K. Sukhanov, V. I. Buné, Y. I. Natarius, V. G. Radchenko, A. I. Savich, and A. A. Khrapkov. 1989. "State of Hydropower Installations in Armenia after the Spitak Earthquake." *Power Technology and Engineering* 23 (8): 450–455. doi: 10.1007/BF01439512.

Li, T. B. 2011. "Damage to Mountain Tunnels Related to the Wenchuan Earthquake and Some Suggestions for Aseismic Tunnel Construction." *Bulletin of Engineering Geology and the Environment* 71 (2): 297–308. doi: 10.1007/s10064-011-0367-6.

The MathWorks. 2010. *MATLAB Signal Processing Toolbox User's Guide*. Natick, MA: The MathWorks.

Wang, Z. Z., B. Gao, Y. J. Jiang, and Y. Song. 2009. "Investigation and Assessment on Mountain Tunnels and Geotechnical Damage after the Wenchuan Earthquake." *Science in China Series E: Technological Sciences* 52 (2): 546–558. doi: 10.1007/s11431-009-0054-z.

Wang, W. L., T. T. Wang, J. J. Su, C. H. Lin, C. R. Seng, and T. H. Huang. 2001. "Assessment of Damages in Mountain Tunnels due to the Taiwan Chi-Chi Earthquake." *Tunnelling and Underground Space Technology* 16 (3): 133–150. doi: 10.1016/S0886-7798(01)00047-5.

Yukio A., and K. Tsutomu. 2003. "Concept of Performance Based Seismic Design Guideline Underground Reinforced Concrete Structures in Nuclear Power Plants in Japan." In *Transactions of the 17th International Conference on Structural Mechanics in Reactor Technology*, Prague, Czech Republic, 17–22 August 2003: 123–131. Raleigh, NC: SMiRT.

Zhang, Y. M., Q. Sheng, Y. H. Zhang, and Z. Q. Zhu. 2009. "Artificial Simulation of Nonstationary Artificial Seismic Motion for Large-scale Underground Cavern Group Located in Alpine Gorge Area." *Rock and Soil Mechanics* 30 (Supp.): 41–46. (in Chinese). doi: 10.3969/j.issn.1000-7598.2009.z1.010.

Zhang, Y. T., M. Xiao, and J. N. Chen. 2010. "Seismic Damage Analysis of Underground Caverns Subjected to Strong Earthquake and Assessment of Post-earthquake Reinforcement Measures." *Disaster Advances* 3 (4): 127–132.

Zhao, B. Y., and Z. Y. Ma. 2009. "Influence of Cavern Spacing on the Stability of Large Cavern Groups in a Hydraulic Station." *International Journal of Rock Mechanics and Mining Sciences* 46 (3): 506–513. doi: 10.1016/j.ijrmms.2008.10.002.